Transcriptome Analysis of the Gene Expression Profiles Associated with Fungal Keratitis in Mice Based on RNA-Seq

Qing Zhang,[1] Jian Zhang,[2] Mengting Gong,[2] Ruolan Pan,[2] Yanchang Liu,[3] Liming Tao,[1] and Kan He[2]

[1]Department of Ophthalmology, The Second Hospital of Anhui Medical University, Hefei, Anhui, People's Republic of China
[2]Center for Stem Cell and Translational Medicine, School of Life Sciences, Anhui University, Hefei, Anhui, People's Republic of China
[3]Department of Orthopedics, The Second Hospital of Anhui Medical University, Hefei, Anhui, People's Republic of China

Correspondence: Liming Tao, Department of Ophthalmology, The Second Hospital of Anhui Medical University, 678 Furong Road, Hefei, Anhui 230601, People's Republic of China; taolimingchina@163.com.
Kan He, Center for Stem Cell and Translational Medicine, School of Life Sciences, Anhui University, 111 Jiulong Road, Hefei 230601, Anhui, People's Republic of China; hekan_803@163.com.

Received: October 26, 2019
Accepted: May 8, 2020
Published: June 15, 2020

Citation: Zhang Q, Zhang J, Gong M, et al. Transcriptome analysis of the gene expression profiles associated with fungal keratitis in mice based on RNA-Seq. *Invest Ophthalmol Vis Sci.* 2020;61(6):32. https://doi.org/10.1167/iovs.61.6.32

Purpose. Fungal keratitis (FK) is an eye disease that can lead to blindness and has a high incidence worldwide. At present, there is no effective treatment for this disease. There are innate immune response mechanisms that protect against fungal infections. One example is C-type lectin receptors (CLRs), which can identify fungal invaders and trigger signal transduction pathways and cellular responses to eliminate pathogens. However, previous studies have focused mostly on single-receptor factors, and a systematic analysis of the genetic factors underlying the pathogenesis of FK has not been conducted. This study aimed to investigate the molecular mechanisms of FK in terms of genomics and to further elucidate its pathogenesis.

Methods. We performed a transcriptome analysis of a mouse model of FK using RNA sequencing to obtain the relevant gene expression profiles and to identify differentially expressed genes, signaling pathways, and regulatory networks of the key genetic factors in the pathogenesis of murine FK.

Results. Several genes that are significantly associated with FK and serve as markers of FK, such as the inflammatory cytokine genes *IL1B*, *IL6*, *IL10*, *IL23*, and *TNF*, were identified. The mRNA and protein expression patterns of IL-1β, IL-6, and TNF-α in the corneas of mice with FK were validated by quantitative RT-PCR and Luminex multiplex assay technology. The Wnt, cGMP–PKG, and Hippo signaling pathways were significantly enriched during fungal infection of mouse corneas.

Conclusions. Our study may help to elucidate the mechanisms of FK pathogenesis and to identify additional candidate drug targets for the treatment of FK.

Keywords: fungal keratitis, RNA sequencing, signaling pathways, gene, pathogenesis

Fungal keratitis (FK) is a severe corneal infection that can lead to blurred vision, blindness, and redness and pain in the eyes that do not improve when contact lenses are removed.[1,2] Compared with the incidence in temperate regions, the incidence of FK is higher in tropical and subtropical regions. FK is more common in hot and humid climates and in tropical areas with large populations engaged in agriculture, such as India. The spectrum of FK in southern Florida in the United States was regularly reported to be most commonly caused by *Aspergillus* and *Fusarium* spp.[3,4] The prevention and treatment of FK are major challenges that can be solved by studying the pathological characteristics of FK.

In the process of fungal infection and invasion, the first key step of an effective immune response is the identification of invaders by the host. Various pattern recognition receptors (PRRs) on different cell populations recognize fungal invaders and trigger signal transduction pathways and cellular responses, including phagocytosis, respiratory burst, and cytokine and chemokine secretion, with the aim of eliminating the pathogens. The common PRRs include four families: C-type lectin receptors (CLRs), Toll-like receptors (TLRs), RIG-1-like receptors, and nucleotide-binding oligomerization domain-like receptors (NLRs), such as Nod proteins. Each of these receptors is different in terms of ligand recognition, signal transduction, and subcellular localization.[5,6] It has been reported that CLRs, such as Dectin-1, are the main receptors that recognize fungi, and TLRs and NLRs play an auxiliary role.[7] As a component of the fungal cell wall, beta-glucan binds to Dectin-1 on the immune cell membrane and leads to the recruitment of Syk kinase and the formation of CARD protein–BCL-10–MALT1 (CBM) signalosomes.[8,9] The CBM signaling body is an upstream molecule of inflammatory signaling pathways, such as the nuclear factor kappa-light-chain-enhancer of activated B cells (NF-κB) and mitogen-activated protein kinase (MAPK) pathways, which can promote the production and release of inflammatory factors and play important roles in fungal infectious diseases.[10]

Here, we performed a transcriptome analysis of a mouse model of disease based on high-throughput sequencing technology to systematically study the molecular mechanisms that regulate FK. To some extent, this analysis may provide basic support for the diagnosis of patients and the treatment of FK.

Materials and Methods

Fungal Strains and Establishment of the Mouse Model

The strain of *Aspergillus fumigatus* (*A. fumigatus*) was CCTCC AF 93048, which was obtained from the China Center for Type Culture Collection (Wuhan, China). The strain was cultured for 3 to 4 days on potato dextrose agar, and suspensions of fresh conidia were prepared by scraping the conidia from the surface of the medium. The samples were quantified using a hemocytometer and adjusted to a final concentration of 5×10^4 conidia/µl in PBS. C57BL/6 mice (Charles River Laboratories, Beijing, China), 6 to 8 weeks old, were adaptively fed for 1 week and randomly divided into two groups. The corneal epithelium in the experimental group (named the Af group) was scraped, and an *A. fumigatus* spore suspension was injected into the corneal stroma.[11,12] The mice that served as negative controls were mock inoculated with sterile PBS (named the PBS group). Only the right eyes of each mouse in the Af group and PBS group were treated for the experiments. The cornea samples from the Af group at 2 days and 5 days post-injection were labeled Af-2 and Af-5, respectively. The mice were treated in accordance with the ARVO Statement for the Use of Animals in Ophthalmic and Vision Research. The experiments were approved by the Animal Ethics Committee of Anhui Medical University.

Clinical Scoring and Corneal Fungal CFU Analysis in Mice

We randomly selected five mice from each group and scored them. Then, the corneas were excised, and the fungal colony-forming units (CFUs) per cornea were determined. The standard of clinical scoring and CFU analysis were based on a study by Wu et al.[12] A score of 0 to 4 was assigned to each of the following three criteria: area of opacity, density of opacity, and surface regularity. The final corneal pathology score of each mouse was the sum of the three scores described above. Thus, the minimum value was 0, and the maximum value was 12. To assess fungal viability, each cornea was homogenized in 100 µl PBS. Subsequently, serial dilutions were performed and plated onto potato dextrose agar plates. *A. fumigatus* was cultured at 37°C for 3 days.

Histopathology Examinations

The infected corneas treated with either *A. fumigatus* or the control PBS were enucleated from the euthanized mice, fixed in 4% paraformaldehyde, and then embedded in paraffin. Sections (4 µm) were cut and stained with hematoxylin and eosin (H&E) for general histological analysis. Gomori methenamine silver (GMS) staining was performed to identify the fungal hyphae and spores.

Immunohistochemistry

Corneal paraffin sections with thicknesses of 4 µm were used. Immunohistochemistry was performed by using the 3,3′-diaminobenzidine staining method. The endogenous peroxidase was inactivated by incubating the sections with 3% H_2O_2 for 20 minutes. The rabbit anti-mouse IL-1β, IL-6, IL-10, IL-23, and TNF-α antibodies (1:200; Bioss, Beijing, China) were applied overnight at 4°C. The sections were washed three times with PBS for 5 minutes each and then incubated with peroxidase-conjugated goat anti-mouse IgG (1:1000; Zsbio, Beijing, China) for 20 minutes at room temperature. PBS buffer was used as a negative control. The cells with brownish-yellow particles in the cytoplasm and cell membrane were considered positive.

Cytokine Analysis

The mouse corneas were excised 2 days and 5 days after injection with *A. fumigatus* or PBS and homogenized in 200 µl of PBS–0.1% Triton X-100 (Sigma-Aldrich, St. Louis, MO, USA). We removed the cellular particles by centrifugation and used the supernatants for cytokine analysis. The concentrations of cytokines, including IL-1β, IL-6, IL-10, IL-23, and TNF-α, were measured using Luminex multiplex assay technology (Thermo Fisher Scientific, Waltham, MA, USA). The plate was read on a Luminex 200TM instrument. The data preprocessing and analysis were conducted using Luminex xPONENT software.

mRNA Extraction and Sequencing

RNA samples were extracted from the resected corneas of the PBS-2, Af-2, and Af-5 groups using TRIzol (Thermo Fisher Scientific) and pooled together within each group. cDNA from each sample was synthesized from 1 µg of total RNA using reverse transcriptase (Takara Biomedical Technology Co., Ltd., Beijing, China) according to the manufacturer's instructions. The preparation of the cDNA library and RNA sequencing were performed by Nanjing Personal Gene Technology Co., Ltd. (Nanjing, Jiangsu, China). The cDNA originating from the RNA fragments was paired and sequenced using the HiSeq X10 high-throughput sequencing platform (Illumina, San Diego, CA, USA), and an average of 6 G reads per sample were obtained. The total RNA was extracted from the cornea samples of the mice in the PBS-2, Af-2, and Af-5 groups, and the quality of the RNA was examined with a 2100 Bioanalyzer (Agilent, Santa Clara, CA, USA). The RNA integrity number values of all the sequencing samples were more than 7.0, and they were 9.2, 8.6, and 8.8 for the PBS-2, Af-2, and Af-5 groups, respectively (Table 1). The sequencing data for the three groups of samples are shown in Table 1. The results show that the Q20 and Q30 quality levels of the three groups of samples were above 95% and 90%, respectively. Our sequencing data are available in the functional genomics database of ArrayExpress (https://www.ebi.ac.uk/arrayexpress/) under accession number E-MTAB-7907.

Differentially Expressed Gene Analysis

We analyzed the RNA-Seq data based on the regular protocol. The data source of the selected reference genome was the Ensembl database (http://www.ensembl.org/). The mouse reference genome of *Mus musculus* GRCm38.dna.fa

Investigative Ophthalmology & Visual Science

Table 1. Quality of Sequencing Samples and Data

Sample	RNA Integrity Number	Reads (n)	Q20 (%)	Q30 (%)	Clean Reads	
					n	%
PBS-2	9.2	70,082,806	97.91	94.75	69,859,772	99.68
Af-2	8.6	76,228,368	97.74	94.37	75,974,668	99.66
Af-5	8.8	75,979,188	97.80	94.52	75,721,772	99.66

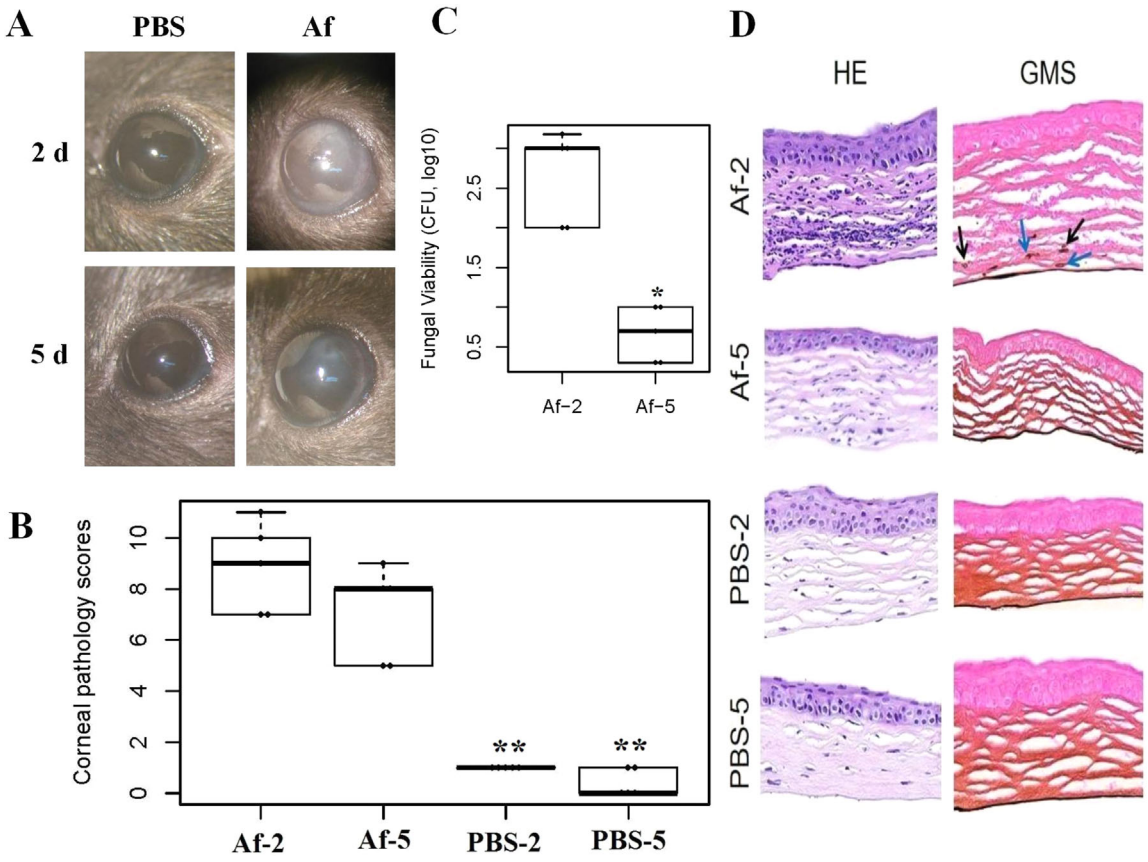

Figure 1. Phenotypic results of the fungal keratitis mouse model. (**A**) The corneal lesions of the mice in the experimental group (Af group) and the control group (PBS group) were observed under a microscope on the second or fifth day. (**B**) The corneal pathology scores were assessed in each group ($^{**}P < 0.01$). (**C**) The fungal viability was assessed in the Af group. The CFUs in the Af-2 group were significantly higher than in the Af-5 group ($^{*}P < 0.05$). **(D)** H&E and GMS staining (400×) was performed in each group. The *black arrow* indicates conidia, and the *blue arrow* indicates hyphae.

was used in this experiment, the size of which was approximately 2.73 GB. First, the raw data were filtered to obtain clean data with high-quality sequences. The reference genome index was established through Bowtie2, and the filtered reads were then compared to the reference genome using TopHat2.[14,15] The htSeqTools software was used to compare the read count values of each gene as the original expression of the gene, and fragments per kilobase million (FPKM) estimation was then used to standardize the expression.[16] Next, we used the Procmp function of R Language 3.5.2 to perform a principal component analysis of each sample according to the amount of expression. Pearson's correlation coefficient was used to describe the correlation of the gene expression levels among the samples. The R Language DESeq software package was used to analyze the differentially expressed genes (DEGs) and the probability of the DEGs.[17] The criteria for screening the DEGs were selected as log2 fold change > 1 and $P < 0.05$. The volcanic maps of the differentially expressed genes were drawn using the R Language ggplots2 software package.

Pathway Enrichment Analysis

We counted the number of differentially expressed genes at different levels of the KEGG pathway (https://www.genome.jp/kegg/pathway.html) and then determined the metabolic pathways and signaling pathways in which the differentially expressed genes were primarily involved.[18] Based on the whole genome, hypergeometric distribution was used to calculate the pathway in which the DEGs were significantly enriched.

Investigative Ophthalmology & Visual Science

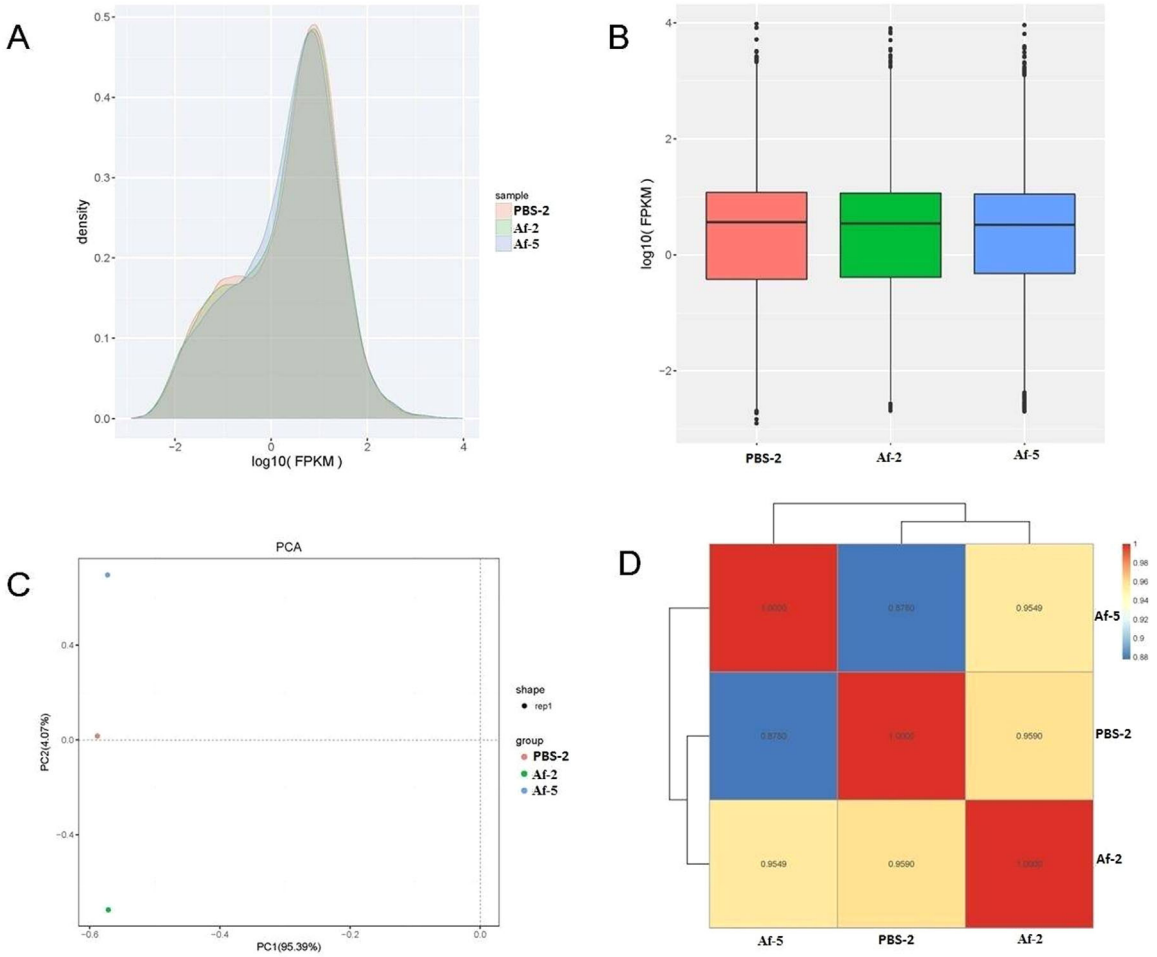

Figure 2. Sequencing data quality control. (**A**) FPKM density distribution of the sequencing data. The *x*-axis represents the log10 (FPKM) value of the gene, and the *y*-axis represents the distribution density of the genes with corresponding expressions. (**B**) Boxplot of the FPKM density distribution. (**C**) Principle component analysis of the sequencing samples. (**D**) Correlation test of the sequencing samples.

Quantitative PCR

Primers for the target genes were designed using Primer 3.0 input software.[19,20] The quantitative PCR (qPCR) experiment was performed with the TransStart Tip Green qPCR SuperMix (Takara). The expression level of each transcript was normalized to that of glyceraldehyde-3-phosphate dehydrogenase and analyzed using the $2^{-\Delta\Delta CT}$ method. All of the experiments were performed in triplicate.

Results and Discussion

Construction and Phenotypic Observation of the Fungal Keratitis Mouse Model

Under the microscope, we observed the corneal lesions of the mice in the experimental group (Af group) and the control group (PBS group), which are shown in Figure 1A. In the control group, the corneas regained the normal appearance on the second day and remained unchanged on the fifth day. In the experimental group, corneal edema aggravated on the second day, showing white porcelain changes, local ulcers, or perforation. On the fifth day in the Af group, the severity of cornea infection was mitigated, and if the area of the ulcer was smaller then there was a trend of scar healing. Compared to those of the PBS groups, the clinical scores of the Af-2 and Af-5 groups were significantly higher, which indicated that the symptoms of fungal keratitis in the Af groups were more severe (Fig. 1B). Based on the assessment of the fungal viability in the Af group, the CFUs in the Af-2 group were found to be significantly higher than in the Af-5 group ($P = 0.029$) (Fig. 1C). Compared with that of the other groups, the corneal stroma in the Af-2 group was heavily infiltrated, according to H&E staining, and fungal hyphae and spores were observed, according to GMS staining (Fig. 1D). These phenotypic results indicate that we successfully constructed a mouse model of fungal keratitis.

Assessment of Sequencing Data Quality

In addition, we detected the expected number of fragments per kilobase of transcript sequence per million reads mapped (FPKM) density and saturation distribution at the transcriptome level in the three groups of sequencing samples. The statistical results of the expression characteristics of all the genes in each sample are shown in Figures 2A and 2B. The results of the principal component analysis and sample correlation tests show that there is clear heterogeneity among the three groups of sequencing samples, as shown in Figures 2C and 2D. The above information shows that

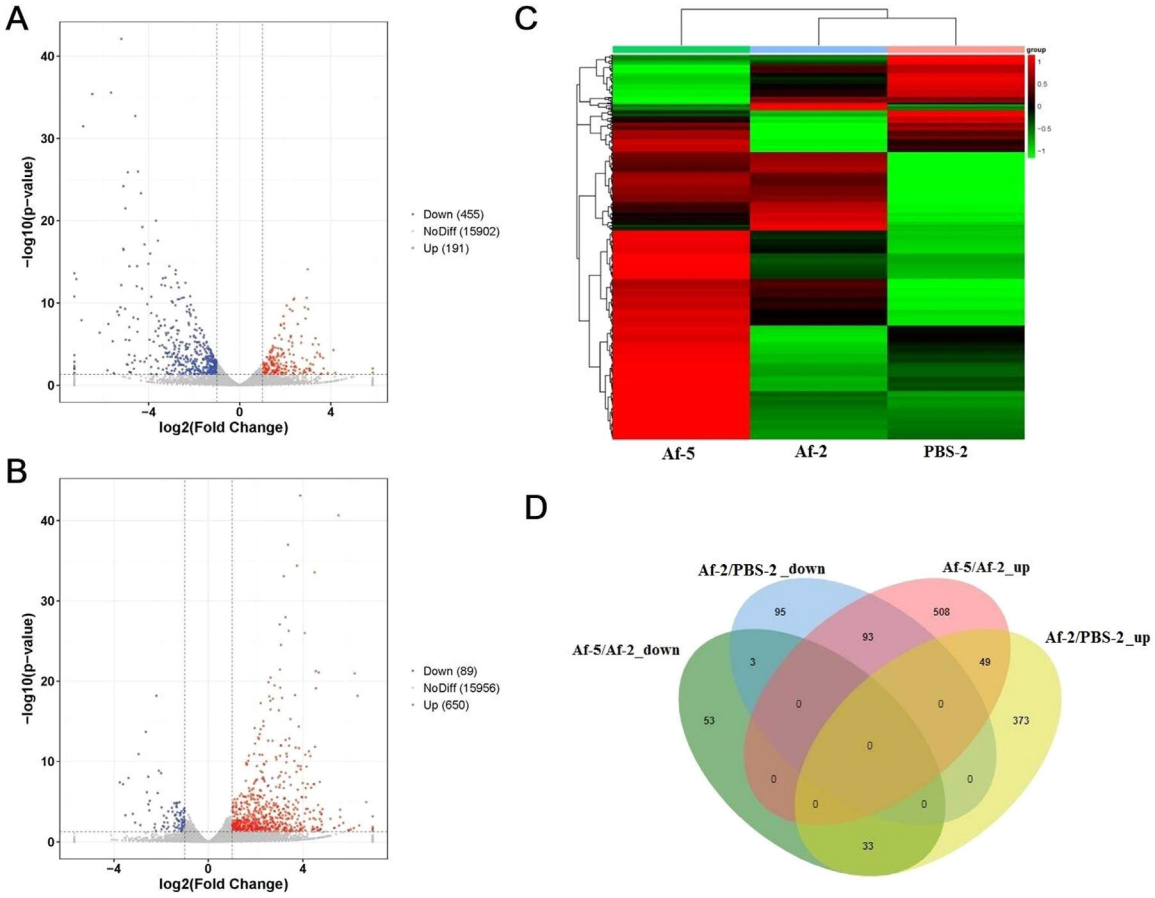

Figure 3. Results of the DEGs associated with fungal keratitis in mice. (**A**) Volcano plot of the significant DEGs between the PBS-2 group and Af-2 group. (**B**) Volcano plot of the significant DEGs between the Af-5 group and Af-2 group. The *x*-axis represents the log2 fold change and the *y*-axis represents –log10 (*P* value) of each significant DEG. (**C**) A heatmap of each significant DEG. **(D)** Comparison of the DEGs at two different time points. The Venn diagram shows the overlapping up- or downregulated DEGs at two different time points.

the high-throughput sequencing data of the three groups of samples are of high quality and meet the requirements for subsequent transcriptomics analysis.

Significant DEGs Associated with Fungal Keratitis in Mice

Based on the alignment with the mouse reference genome, a total of 16,548 transcripts were identified. By comparing the gene expression profiles of the PBS-2 group and Af-2 group (Af-2 group/PBS-2 group), and based on the threshold criterion of log2 fold change > 1 and $P < 0.05$ significance, we screened 646 differentially expressed genes, including 455 upregulated genes and 191 downregulated genes (Fig. 3A). Excluding the factor of zero value, expression of the *SPDEF* (SAM pointed domain-containing Ets transcription factor) gene indicated that it was the most significantly upregulated gene, and this gene was increased 154-fold in the Af-2 group compared to the PBS-2 group. SPDEF, which is a member of the ETS transcription factor family, has been reported to play an important role in conjunctival goblet cell differentiation and pulmonary Th2 inflammation.[21] Among the 191 significantly downregulated genes, expression of the *GALNT15* (polypeptide *N*-acetylgalactosaminyltransferase 15) gene in the Af-2 group was the lowest; the expression of this gene was approximately 57 times lower in the Af-2 group than in the PBS-2 group. However, to the best of our knowledge, there have been no reports on the function of *GALNT15*.

By comparing the gene expression profiles of the Af-5 group and Af-2 group (Af-5 group/Af-2 group), the total number of differentially expressed genes was 739, including 650 upregulated genes and 89 downregulated genes (Fig. 3B). Among the 650 significantly upregulated genes, expression of the *MARCO* (macrophage receptor with collagenous structure) gene in the Af-5 group increased the greatest extent; the expression of this gene was approximately 124 times higher in the Af-5 group than in the Af-2 group. In a study of Cryptococcus *neoformans*-infected mice, it was demonstrated that deficiency of the scavenger receptor MARCO could lead to impaired fungal control during the afferent phase of cryptococcal infection.[22] It was also reported that MARCO might significantly mediate adenovirus infection and the subsequent innate responses in macrophages.[23]

In addition, we further compared the differentially expressed gene sets identified above. A heatmap of the expression patterns of these differentially expressed gene sets is shown in Figure 3C. The comparison of the significantly DEGs at both infection time points showed that there were three commonly downregulated genes, including *GLDC* (glycine decarboxylase), *ALDH1A1* (aldehyde

Table 2. Common DEGs During Fungal Infection in the FK Mouse Model

Regulation	Genes
Af-5/Af-2 downregulated; Af-2/PBS-2 downregulated (n = 3)	*GLDC*, *ALDH1A1*, *PPP1R3C*
Af-5/Af-2 downregulated; Af-2/PBS-2 upregulated (n = 33)	*CCL3*, *MSH6*, *G0S2*, *SLPI*, *CCL4*, *TNFAIP3*, *SRGN*, *SLC26A4*, *RDH12*, *EDN1*, *ACOD1*, *RETNLG*, *SAMSN1*, *DYNAP*, *IFITM3*, *HDC*, *IL1B*, *CELF3*, *CXCL3*, *CXCL1*, *NLRP3*, *LIF*, *LARS2*, *CSF3*, *CCRL2*, *VTCN1*, *CD14*, *HBB-BS*, *IFI205*, *S100A8*, *CXCL2*, *HBA-A2*, *HBA-A1*
Af-5/Af-2 upregulated; Af-2/PBS-2 downregulated (n = 93)	*SERPINF1*, *SLC13A2*, *COL6A1*, *COL1A1*, *PEG3*, *APOE*, *FCGRT*, *AQP1*, *SCARF2*, *ZFP651*, *SCUBE1*, *MATN4*, *PLOD1*, *DPEP1*, *LAMA2*, *DCN*, *KERA*, *COL6A2*, *MRC2*, *CACNA1G*, *FBLN5*, *OGN*, *GALNT15*, *WNT5A*, *APOD*, *P3H3*, *SERPING1*, *SMOC2*, *ADAMTS10*, *PDGFRB*, *ZFHX4*, *ITIH5*, *TFAP2B*, *COL5A2*, *DPT*, *RGS5*, *DNM1*, *COL5A1*, *ADAM33*, *POSTN*, *OLFML3*, *COL11A1*, *DKK2*, *COL24A1*, *MXRA8*, *SPARCL1*, *COL1A2*, *PCOLCE*, *A2M*, *MGP*, *CPXM2*, *ITM2A*, *SRPX2*, *BGN*, *FGFR1*, *NKD1*, *CDH11*, *MMP2*, *BMPER*, *ITGA11*, *LOXL1*, *PTH1R*, *ITGBL1*, *PODXL2*, *TNXB*, *LUM*, *ADAMTS2*, *CPZ*, *DCHS1*, *ISLR*, *LMX1B*, *IGFBP2*, *KCNS1*, *SLC26A7*, *COL16A1*, *PIEZO2*, *FMOD*, *PRELP*, *KIRREL*, *MFAP4*, *POU3F3*, *PENK*, *COL27A1*, *OLFML2A*, *COL6A3*, *CEMIP*, *CYP2F2*, *JAM2*, *NTRK2*, *TNS1*, *COL8A2*, *CPED1*, *SRPX*
Af-5/Af-2 upregulated; Af-2/PBS-2 upregulated (n = 49)	*ITGB2*, *CFP*, *CYP2A5*, *CYBB*, *MMP9*, *CCL9*, *MOXD1*, *GABRP*, *IGFBP3*, *NCKAP1L*, *ADAMTS1*, *CLEC4N*, *MYO1F*, *TMEM173*, *CASP12*, *COL3A1*, *IL1R2*, *FCGR2B*, *TNC*, *LAPTM5*, *SORCS2*, *PF4*, *ITGAX*, *ST3GAL4*, *CAR12*, *PLOD2*, *NT5E*, *LTF*, *SCARA3*, *ACTA2*, *SERPINE1*, *CTSS*, *SECTM1B*, *SH3KBP1*, *SERPINA3G*, *SPRR2D*, *PIGZ*, *MMP12*, *KLK13*, *H2-EB1*, *KCNJ15*, *PI15*, *LYZ2*, *CSN1S1*, *H2-AB1*, *SPRR2A3*, *4833423E24RIK*, *CLEC7A*, *B3GNT7*

dehydrogenase family 1, subfamily A1), and *PPP1R3C* (protein phosphatase 1, regulatory subunit 3C). There were 49 commonly upregulated genes in both groups, such as *CASP12* (caspase 12) and *IL1R2* (interleukin 1 receptor, type II). Interestingly, 33 genes, including the *IL1B* gene, were upregulated in the comparison of Af-2/PBS-2 but downregulated in the comparison of Af-5/Af-2. A total of 93 genes, including the *WNT5A* gene (wingless-type MMTV integration site family, member 5A), were downregulated in the comparison of Af-2/PBS-2 but upregulated in the comparison of Af-5/Af-2. The details of the results described above are shown in Figure 3D and Table 2. Most of these commonly identified genes have been reported in previous studies of fungal ophthalmopathy or immunology. IL-1α and IL-1β are two types of IL-1, which is a cytokine that is produced by monocytes, endothelial cells, fibroblasts, and other types of cells in response to infection that bind to the same receptor of the immunoglobulin superfamily. Previous studies have shown that IL-1β derived from neutrophils participates in corneal antifungal responses and immune defense as an important proinflammatory factor.[24] IL-1β production can be induced by fungal infection in the mouse cornea, and this production can be regulated by the Dectin-1/Syk pathway.[25] Casp11 and Casp1 participate in the modification of IL-1β from its precursor to mature form.[26,27] Wnt5a is a secretory glycoprotein and a member of the highly conserved Wnt protein family. *WNT5A* expression regulation and signal transduction are closely related to the inflammatory response, suggesting that *WNT5A* and its signaling pathway play an important role in the occurrence and development of inflammatory diseases. According to in vivo and in vitro experiments, *WNT5A* was identified as a critical component of the antifungal immune response that can produce Dectin-1- and LOX-1-induced inflammatory signatures in response to *A. fumigatus* infection.[28] Caspase-12 may play an important role in the process of hypersensitivity to oxidative stress in keratoconus (KT) cornea fibroblasts.[29] Through analysis of gene expression profile data, *GLDC* was identified as playing a significant role in regulating various inflammatory processes.[30,31] Aldehyde dehydrogenase (ALDH1A1) was found to be expressed in immature monocyte-derived dendritic cells; ALDH1A1 is an enzyme that contributes to the production of retinoic acid and is an important immunomodulator that regulates HIV-1 replication.[32]

In fact, some previous studies have described the host transcriptional response to fungi. In a study by Kale et al.,[33] the host transcriptomic response to *A. fumigatus* infection was described in a murine pulmonary model. Notable differences in host gene expression at the interface of immunity and metabolism have been found between chemotherapeutic and steroid-treated models of mice with invasive pulmonary aspergillosis. We compared our results of 646 DEGs in Af-2/PBS-2 with the 672 immunologically relevant DEGs identified by Kale et al.,[33] and there were 99 overlapping genes. In the study by Wang et al.,[34] gene profiling of murine corneas challenged with *A. fumigatus* was performed by microarray to detect the primary responsive genes during the onset of fungal keratitis. As a result, 61 genes that were upregulated and 48 genes that were downregulated in response to *A. fumigatus* infection were identified from a total of 18,335 genes by array; these genes included some host defense genes, such as *IL3*, *MBL-A*, and *PSGD*. By comparison, 14 common genes were identified in both the microarray-based results and RNA-Seq data. These comparison results are shown in Supplementary Table S1. In this study, we employed RNA sequencing not only to characterize host gene expression in a murine model of FK but also to reveal the dynamic expression patterns.

Significantly Enriched Pathways Associated with Fungal Keratitis in Mice

Based on the method of gene enrichment analysis, we identified the significantly enriched signal transduction pathways related to the pathogenesis of fungal keratitis in mice. The Af-2/PBS-2-related signal transduction pathway enrichment results are shown in Table 3, and the Af-5/Af-2-related results are shown in Table 4.

Table 3. Enrichment Results of Signal Transduction-Related Pathways in the Af-2/PBS-2 Comparison

Signaling Pathway	FDR	Downregulated Genes, n	Upregulated Genes, n	Downregulated Genes	Upregulated Genes
TNF	2.32E-11	0	24	—	*EDN1*, *CXCL2*, *CXCL3*, *NOD2*, *ICAM1*, *TNFAIP3*, *BIRC3*, *TRAF1*, *BCL3*, *CEBPB*, *MMP9*, *FAS*, *IL18R1*, *LIF*, *TNF*, *MAPK11*, *IL6*, *PTGS2*, *CSF1*, *TNFRSF1B*, *IL1B*, *CXCL1*, *SOCS3*, *NFKBIA*
NF-κB	2.66E-05	1	14	*CARD14*	*LYN*, *RELB*, *CCL4*, *ICAM1*, *TNF*, *TNFAIP3*, *BIRC3*, *PTGS2*, *TRAF1*, *IL1B*, *CD14*, *BCL2A1A*, *BLNK*, *NFKBIA*
PI3K-Akt	3.86E-05	14	17	*TNXB*, *COL1A1*, *COL6A2*, *FGFR1*, *ITGA11*, *PDGFRB*, *COL6A1*, *CCND2*, *NTRK2*, *COL1A2*, *COL6A3*, *EFNA3*, *FGF10*, *LAMA2*	*OSM*, *PIK3R5*, *PIK3AP1*, *NR4A1*, *SPP1*, *CSF3*, *ITGB6*, *THBS1*, *PDGFB*, *CSF3R*, *TNC*, *IL4RA*, *CSF1*, *IL3RA*, *IL6*, *JAK2*, *IL7R*
JAK–STAT	7.70E-05	2	17	*CCND2*, *PDGFRB*	*IL13RA1*, *OSM*, *IFNGR1*, *CSF2RB2*, *CSF3*, *LIF*, *PDGFB*, *IL10RA*, *CSF3R*, *IL4RA*, *IL6*, *IL3RA*, *JAK2*, *SOCS3*, *IL7R*, *CSF2RB*, *IL20RA*
MAPK	2.03E-03	6	17	*CACNA1G*, *NTRK2*, *EFNA3*, *FGF10*, *FGFR1*, *PDGFRB*	*RELB*, *DUSP1*, *NR4A1*, *DUSP5*, *CD14*, *GADD45A*, *IL1A*, *GADD45G*, *FAS*, *GADD45B*, *RAC2*, *PDGFB*, *RASGRP1*, *TNF*, *MAPK11*, *CSF1*, *IL1B*
Rap1	1.46E-02	6	10	*RAPGEF3*, *GNAO1*, *EFNA3*, *FGF10*, *FGFR1*, *PDGFRB*	*ITGB2*, *THBS1*, *RAC2*, *ITGAM*, *PDGFB*, *LCP2*, *MAPK11*, *CSF1*, *APBB1IP*, *FPR1*
HIF-1	3.54E-02	0	9	—	*EDN1*, *TIMP1*, *HMOX1*, *IFNGR1*, *SERPINE1*, *IL6*, *CYBB*, *HK3*, *NOS2*

Table 4. Enrichment Results of Signal Transduction-Related Pathways in the Af-5/Af-2 Comparison

Signaling Pathway	FDR	Downregulated Genes, n	Upregulated Genes, n	Downregulated Genes	Upregulated Genes
PI3K-Akt	4.05E-09	1	42	*CSF3*	*TNN, ITGA1, TNXB, KDR, FLT4, ITGA11, NTRK2, ITGA7, COL6A6, GNB4, RELN, TEK, COL4A6, PDGFRA, CSF1R, PDGFRB, CREB3L1, TNC, COL1A2, IGF1, ITGB3, LAMA2, THBS2, COL1A1, COL4A2, FGFR1, F2R, LAMA4, COL4A1, ITGA4, FN1, FGFR3, COL6A2, ITGA9, COL6A1, COL4A4, COL4A3, PDGFC, FLT1, COL6A3, ITGA5, VWF*
MAPK	3.58E-03	4	21	*CD14, IL1B, DUSP7, RASGRF1*	*CACNA1G, KDR, FLT4, FGFR1, ARRB1, NTRK2, CACNA1C, TGFBR2, MEF2C, TEK, PDGFRA, FGFR3, IL1R1, CSF1R, PDGFRB, TGFB2, FLNC, FLT1, PDGFC, IGF1, TGFB3*
TNF	1.15E-02	7	5	*TNFAIP3, EDN1, IL1B, CXCL1, LIF, CXCL2, CXCL3*	*GM5431, VCAM1, MMP3, CREB3L1, MMP9*
Rap1	2.90E-02	0	17	—	*ADCY7, KDR, ARAP3, FLT4, FGFR1, F2R, TEK, ITGB2, PDGFRA, FGFR3, CSF1R, PDGFRB, ADCY4, FLT1, PDGFC, IGF1, ITGB3*
Wnt	3.62E-02	1	12	*FOSL1*	*FZD2, WISP1, SERPINF1, NFATC4, DKK2, NKD1, WNT11, SOX17, AXIN2, NKD2, SFRP2, WNT5A*
cGMP–PKG	4.10E-02	0	14	—	*MEF2C, MYL9, ADCY7, ATP1A3, EDNRA, CREB3L1, PDE3A, ADCY4, NFATC4, EDNRB, NPR2, ADRA2A, CACNA1C, ATP2B4*
Hippo	4.27E-02	0	13	—	*ITGB2, FZD2, CTGF, TEAD2, SERPINE1, TGFB2, TRP73, WNT11, DLG4, TGFB3, AXIN2, WNT5A, TGFBR2*

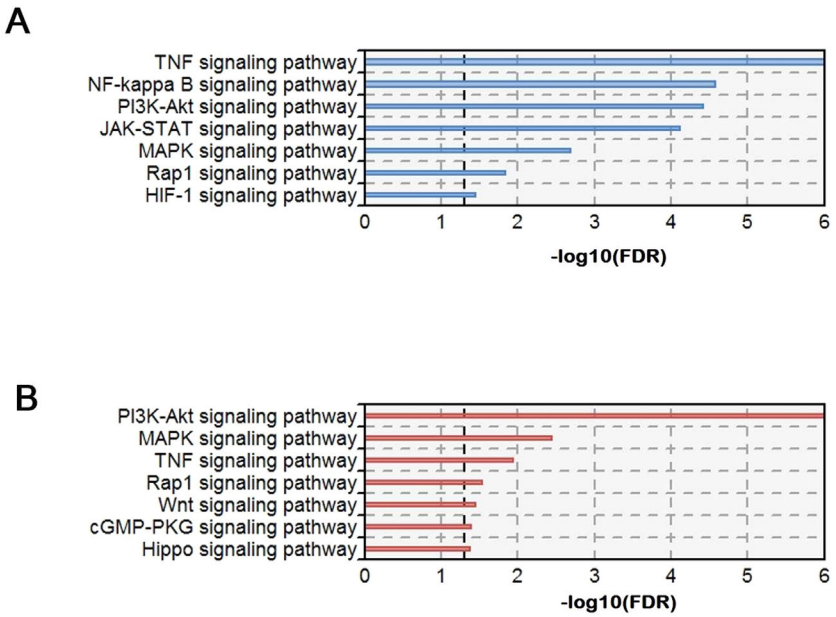

Figure 4. Signal transduction-related pathways enriched at different time points. (**A**) Significant signal transduction-related pathways were enriched in the comparison between the PBS-2 and Af-2 groups. (**B**) Significant signal transduction-related pathways were enriched in the comparison between the Af-5 and Af-2 groups. The *x*-axis represents –log10 (FDR), and the *y*-axis represents the name of each pathway.

Compared to the control group, the experimental group revealed seven different signaling pathways that were significantly involved in the pathogenesis of murine keratitis on the second day of fungal infection (seen in Table 3 and Fig. 4A). According to the significance level, the pathways included the TNF signaling pathway (false discovery rate [FDR] = 2.32E-11), NF-κB signaling pathway (FDR = 2.66E-05), phosphatidylinositol 3-kinases (PI3K)–Akt signaling pathway (FDR = 3.86E-05), Janus kinase (JAK)–signal transducers and activators of transcription (STAT) signaling pathway (FDR = 7.70E-05), MAPK signaling pathway (FDR = 2.03E-03), Rap1 signaling pathway (FDR = 1.46E-02), and hypoxia-inducible factor 1 (HIF-1) signaling pathway (FDR = 3.54E-02). The details of the dysregulated genes in each significantly associated signaling pathway in the comparison of Af-2/PBS-2 are shown in Table 3.

It has been reported that crosstalk of the TGF-β and NF-κB signaling pathways may enhance corneal epithelial senescence through the RNA stress response.[35] TNF-α can inhibit the expression of CX43 and GJIC in human corneal fibroblasts; this inhibition is mediated by the c-Jun N-terminal kinase (JNK) signaling pathway and may play an important role in corneal inflammation.[36] Activating or inhibiting the signal transduction pathways related to the proliferative potential and phenotype maintenance of corneal endothelial cells has been considered an important research direction for the development of new therapies for corneal endothelial dysfunction.[37] In a previous study conducted in corneal peripheral vascular endothelial cells and a mouse model, the occurrence and development of fungal keratitis could be inhibited by IL-17, which suppressed CX43 expression through the Akt signaling pathway.[38] Therefore, corneal endothelial cell dysfunction might play a role in the pathogenesis of fungal keratitis and might be regulated by the identified targets through associated signaling pathways. It has been confirmed in rabbit models that the combined activation of PI3K/Akt and Smad2 leads to the expansion of phenotypic and functional corneal endothelial cells in vitro and expanded cells contribute to the recovery of corneal endothelium.[39] These findings may provide a new method for treating corneal endothelial diseases. The MAPK signaling pathway family is widely distributed in eukaryotic cells and has been associated with a variety of extracellular signals or stimuli, especially inflammatory responses. The physiological response mediated by the MAPK signaling pathway contributes to the progression and healing of ocular trauma.[40] The effect of JAK/STAT inhibitors on the activity of IL-17-producing neutrophils impaired reactive oxygen species production and fungicidal activity but also inhibited elastase and gelatinase activity, which may lead to tissue damage.[41] Rap1 (telomere repeat binding factor 2 interacting protein) has been found to be a regulator of NF-κB, whose deficiency contributes to corneal recovery after injury and may lead to the design of specific NF-κB inhibitors in the treatment of ocular injury.[42] Hypoxia or decreased oxygen tension is considered to be the core of the pathogenesis of neovascular and degenerative diseases of the eye. Previous studies have reported a new mechanism by which hypoxia induces CD36 expression by activating the HIF-1 and PI3K pathways.[43] HIF-1 directly upregulates expression of the inhibitory Per/Arnt/Sim (PAS) domain protein (*IPAS*) gene through a mechanism other than RNA splicing, providing additional gene regulation via negative feedback for the adaptive response under hypoxic/ischemic conditions.[44] In hypoxia-exposed corneal cells, the high expression of cystic fibrosis transmembrane conductance regulator and basal activity of NF-κB may increase the susceptibility to keratitis.[45]

Compared with the second day, the fifth day of fungal infection revealed seven different signaling pathways that were significantly enriched in the pathogenesis of keratitis in mice (shown in Table 4 and Fig. 4B). These pathways were the PI3K–Akt signaling pathway (FDR = 4.05E-09),

Investigative Ophthalmology & Visual Science

MAPK signaling pathway (FDR = 3.58E-03), TNF signaling pathway (FDR = 1.15E-02), Rap1 signaling pathway (FDR = 2.90E-02), Wnt signaling pathway (FDR = 3.62E-02), cGMP-cGMP-dependent protein kinase (PKG) signaling pathway (FDR = 4.10E-02), and Hippo signaling pathway (FDR = 4.27E-02). The first four signaling pathways involved in this stage were common to the previous stage, whereas the latter three signaling pathways were unique to this stage. The details of the dysregulated genes in each significantly associated signaling pathway in the comparison of Af-5/Af-2 are shown in Table 4. Corneal epithelial stratification in mice is the result of the coordinated development of mesenchymal epithelial interactions. It has been shown that the interaction between the Wnt/β-catenin/bone morphogenetic protein 4 (BMP4) axis in the stroma and BMP4/P63 signaling in the epithelium may play a key role in corneal epithelial stratification.[46] To better understand the factors that lead to KT corneas, the researchers used RNA sequencing to conduct a comprehensive transcriptome analysis of human KT corneas. The results showed that the collagen synthesis and maturation pathways were widely disrupted, and the core elements of the TGF-β, Hippo and Wnt signaling pathways were significantly downregulated in the corneal tissue.[47] KCa3.1 (IK1/SK4/KCNN4) is widely expressed in the congenital and adaptive immune systems. KCa3.1/IK1 channels regulated by PKG can form a new immune regulatory feedback system in microglia.[48] In summary, the disease severity of mice was alleviated on the fifth day of fungal infection due to the immune function of the mice, which could be improved by the reduction in proinflammatory gene expression on day 5.

Table 5. qPCR Primers for Inflammatory Cytokines

Genes	Forward Primers	Reverse Primers
IL1B	tccagctacgaatctccgac	aggtgctcaggtcattctcc
IL6	ccctgacccaaccacaaatg	ctacatttgccgaagagccc
IL10	aagctgagaaccaagaccca	aagaaatcgatgacagcgcc
IL23	tgagaagctgctaggatcgg	aggcttggaatctgctgagt
TNF-alpha	cctcagcctcttctccttcc	agatgatctgactgcctggg
WNT5A	tgcggagacaacatcgacta	aagttcatgaggatgcgtgc
TNXB	gaccaccaccatcttcctca	ccaaccacctccatcagtct
COL6A1	gctacaatggatggctggtg	gttctgtgtgggtgggagta
COL6A2	ggtcctctttctgtgctcct	agtggtggagatgtctggtg
COL6A3	gcaatgcatgagaccctctg	actcaaggcccttctgactc
COL1A2	cccgttggcaaagatggtag	accttggctaccctgagaac

Validation of the Expression Patterns of Inflammatory Cytokines

Furthermore, we selected some inflammatory cytokines, including IL-1β, IL-6, IL-10, IL-23 and TNF, and used qPCR to validate their gene expression patterns in mouse corneas during fungal infection. The qPCR primers for all of the selected target genes are shown in Table 5. The qPCR results of the different samples are shown in Figure 5. The expression patterns of these inflammatory cytokine genes in the

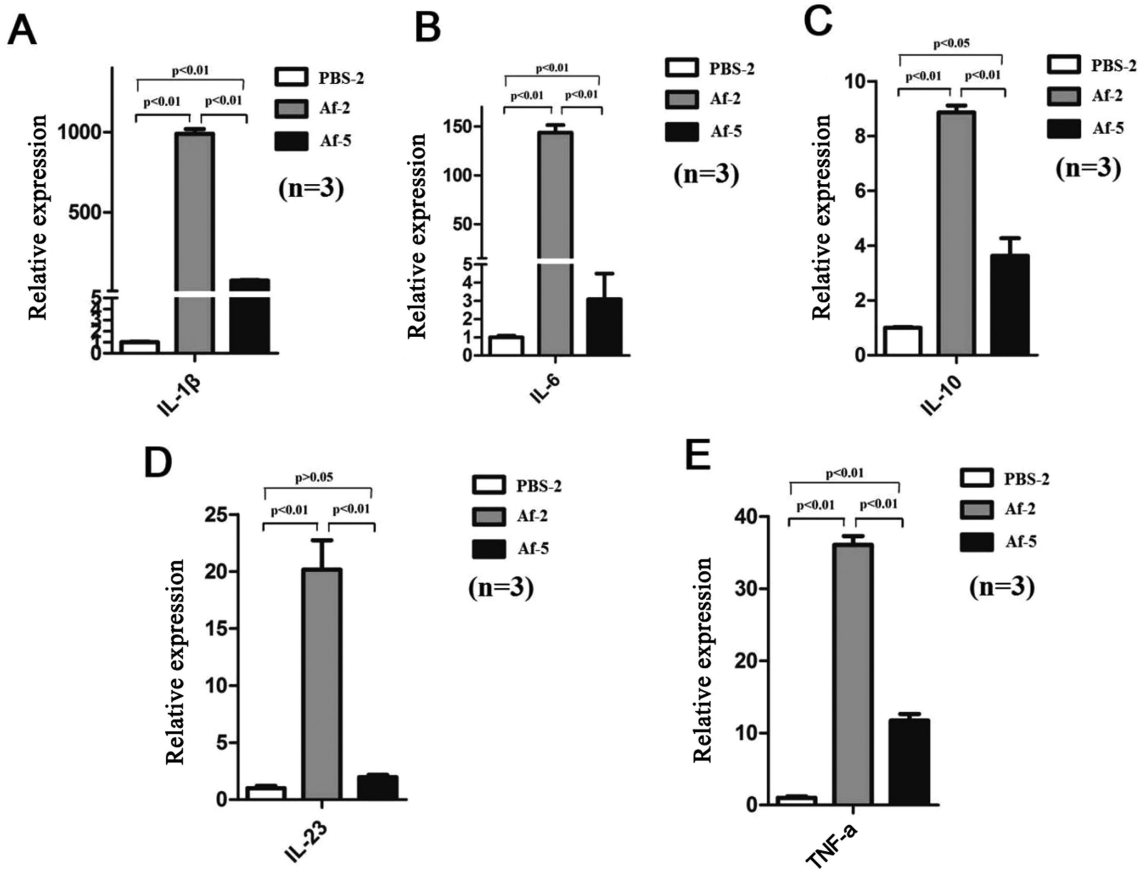

Figure 5. Gene expression patterns of inflammatory cytokines revealed by qPCR. The expression patterns of five inflammatory cytokine genes, including *IL1B* (**A**), *IL6* (**B**), *IL10* (**C**), *IL23* (**D**), and *TNF-α* (**E**), were validated by qPCR. The experiment was performed in triplicate for each group and was repeated three times. The *x*-axis represents three groups: PBS-2, Af-2, and Af-5. The *y*-axis represents the relative expression of each gene in the different groups. The gene expression value in PBS-2 was set to 1.

Investigative Ophthalmology & Visual Science

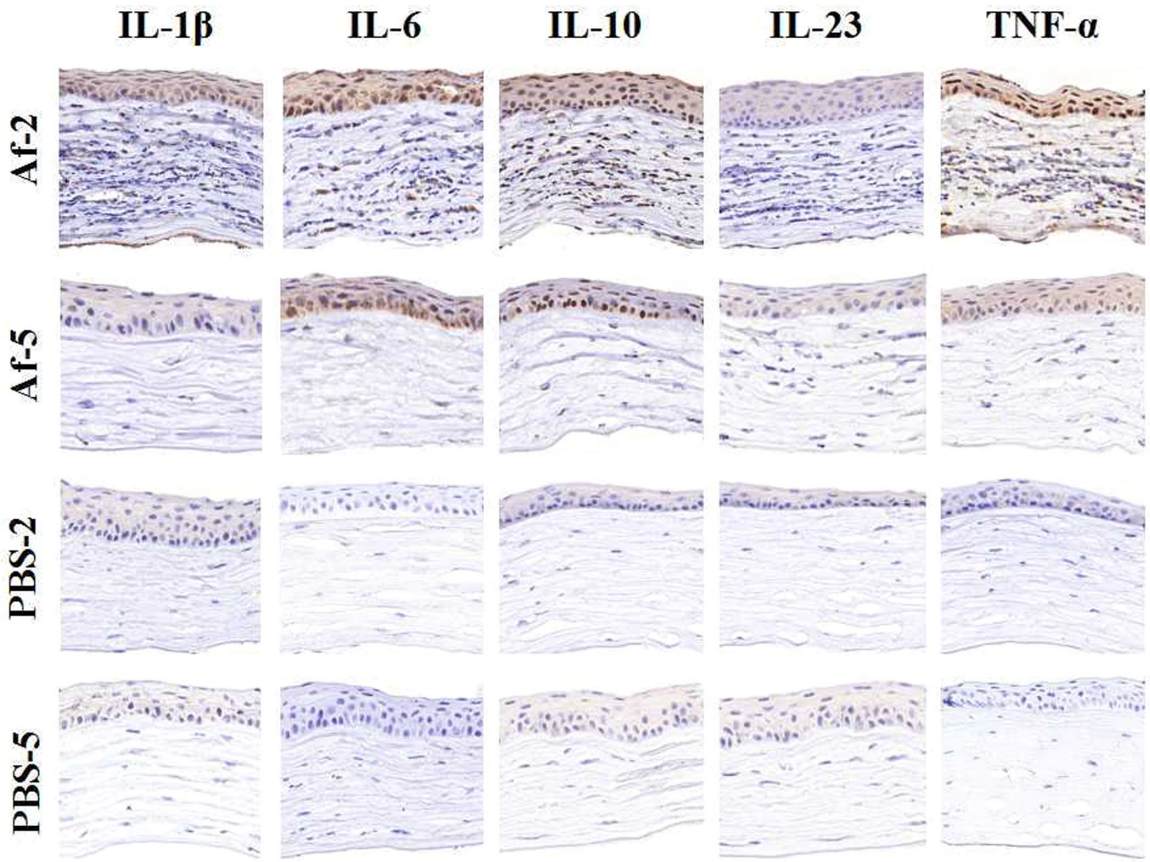

Figure 6. Cytokine expression in mouse corneas evaluated by immunohistochemistry. The expression of five inflammatory cytokines, including IL-1β, IL-6, IL-10, IL-23, and TNF-α, in each group was assessed by immunohistochemistry.

corneal tissue of mice changed significantly during fungal infection. No inflammation was observed in the control group based on the low cytokine gene expression and the lack of obvious corneal opacity. On the second day of fungal infection, the expression of these cytokines reached the highest peak (some, such as the *IL1B* gene, even increased thousands of times). On the fifth day of infection, the expression of these genes showed a downward trend. Each of these inflammatory cytokine genes displayed the same pattern of expression, which included a peak at day 2 of infection and a decrease by day 5 of infection.

The changes in the corneas of the mice mouse at different time points after fungal or PBS injection were observed by immunohistochemistry. As shown in Figure 6, inflammatory cytokines, such as IL-1β, IL-6, IL-10, and TNF-α but not IL-23, were abundant in the Af groups. These cytokines were mainly expressed in the cytoplasm of the corneal epithelial and stromal cells. The expression of five inflammatory factors was detected in the Af and PBS groups at different time points by using the Luminex multiplex assay technology (Fig. 7). The concentration of IL-23 in the cornea was lower than the minimum limit of detection of the chip, so the value could not be obtained. On the second day of fungal infection, the expression of IL-1β, IL-6, IL-10, and TNF-α increased. Compared with that in the Af-5 and PBS-2 groups, the expression of IL-1β, IL-6, and TNF-α, but not IL-10, in the Af-2 group was significantly different ($P < 0.05$). In summary, the cytokine expression patterns of IL-1β, IL-6, and TNF-α were consistent with the results obtained by qPCR. These three inflammatory cytokines can be further used as candidate targets for the treatment of fungal keratitis.

Conclusion

Based on our transcriptome analysis of fungal keratitis in mice by RNA-Seq, we identified a variety of significant signal transduction pathways and their targets. In particular, some inflammatory cytokines, such as IL-1β, IL-6, and TNF-α, and pathways, such as the Wnt, cGMP–PKG, and Hippo signaling pathways, were significantly associated with the pathogenesis of fungal infection in the murine cornea. Targeting these genes and pathways may be useful for the treatment of fungal keratitis.

Acknowledgments

Supported by grants from the Key University Science Research Project of Anhui Province (KJ2017A021), Natural Science Foundation Project of Anhui Province (1508085QC63 and 1908085MC87), Scientific Research Foundation and Academic and Technology Leaders Introduction Project, 211 Project of Anhui University (10117700023), and the Student Research Training Programme of Anhui University (J10118520218 and J10118520307). This work was also supported by the Natural Science Foundation Project of Anhui Medical University (2018xkj042), NSFC Incubation Project of Second Hospital of Anhui Medical University (2019GQFY04), and Science and

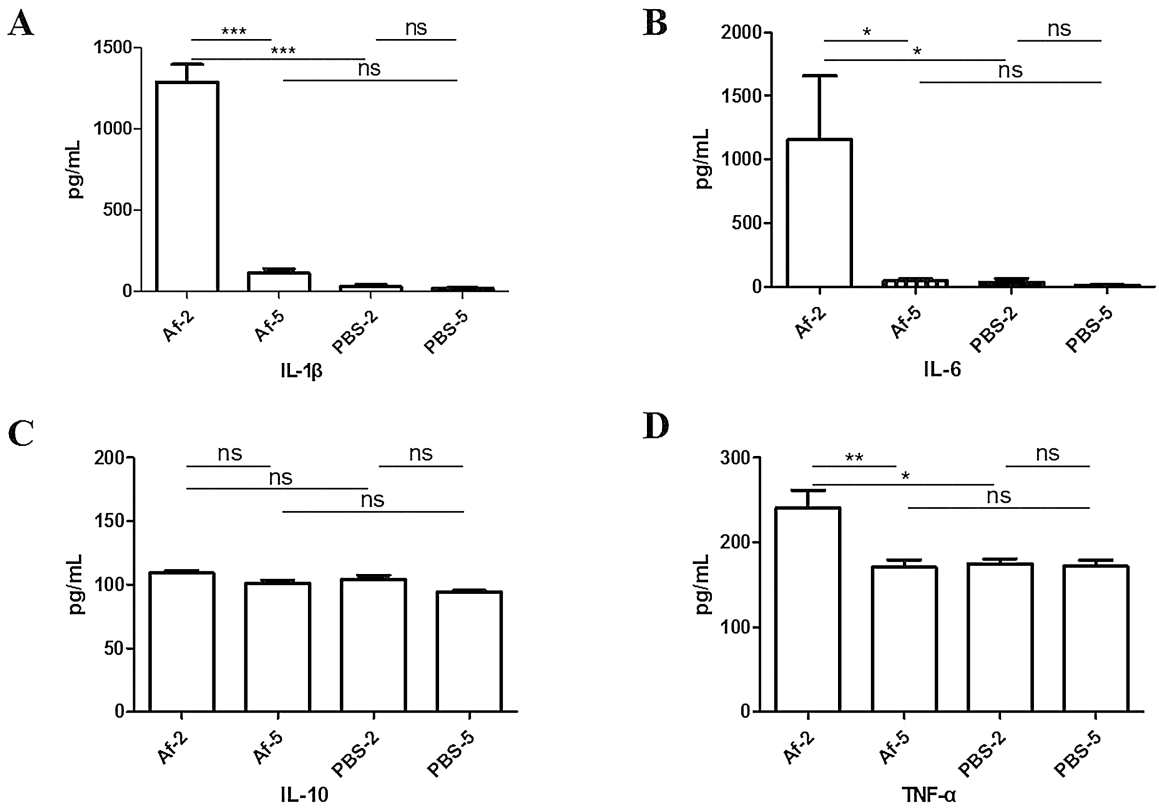

Figure 7. Cytokine expression in fungal keratitis-infected mice tested by multiplex assay. The expression of cytokines, including IL-1β (**A**), IL-6 (**B**), IL-10 (**C**), and TNF-α (**D**), in the Af-2 and Af-5 groups (n = 5 mice in each group) and in the PBS-2 and PBS-5 groups (n = 5 mice in each group) was measured by Luminex multiplex assay technology. The significance level was determined by one-way ANOVA tests ($^{***}P < 0.001$, $^{**}P < 0.01$, $^{*}P < 0.05$).

Technology New Star Training Project of Second Hospital of Anhui Medical University (2018KA08).

Disclosure: **Q. Zhang**, None; **J. Zhang**, None; **M. Gong**, None; **R. Pan**, None; **Y. Liu**, None; **L. Tao**, None; **K. He**, None

References

1. Poggio EC, Glynn RJ, Schein OD, et al. The incidence of ulcerative keratitis among users of daily-wear and extended-wear soft contact lenses. *N Engl J Med*. 1989;321:779–783.
2. Thomas PA. Fungal infections of the cornea. *Eye*. 2003;17:852–862.
3. Liesegang TJ, Forster RK. Spectrum of microbial keratitis in South Florida. *Am J Ophthalmol*. 1980;90:38–47.
4. Rosa RH, Jr, Miller D, Alfonso EC. The changing spectrum of fungal keratitis in south Florida. *Ophthalmology*. 1994;101:1005–1013.
5. Inui M, Kikuchi Y, Aoki N, et al. Signal adaptor DAP10 associates with MDL-1 and triggers osteoclastogenesis in cooperation with DAP12. *Proc Natl Acad Sci U S A*. 2009;106:4816–4821.
6. Zelensky AN, Gready JE. The C-type lectin-like domain superfamily. *FEBS J*. 2005;272:6179–6217.
7. Sancho D, Reis e Sousa C. Signaling by myeloid C-type lectin receptors in immunity and homeostasis. *Annu Rev Immunol*. 2012;30:491–529.
8. Brown GD, Gordon S. Immune recognition. A new receptor for beta-glucans. *Nature*. 2001;413:36–37.
9. Ruland J, Hartjes L. CARD-BCL-10-MALT1 signalling in protective and pathological immunity. *Nat Rev Immunol*. 2019;19:118–134.
10. Drummond RA, Saijo S, Iwakura Y, Brown GD. The role of Syk/CARD9 coupled C-type lectins in antifungal immunity. *Eur J Immunol*. 2011;41:276–281.
11. Tarabishy AB, Aldabagh B, Sun Y, et al. MyD88 regulation of *Fusarium* keratitis is dependent on TLR4 and IL-1R1 but not TLR2. *J Immunol*. 2008;181:593–600.
12. Wu TG, Wilhelmus KR, Mitchell BM. Experimental keratomycosis in a mouse model. *Invest Ophthalmol Vis Sci*. 2003;44:210–216.
13. Zhao G, Zaidi TS, Bozkurt-Guzel C, et al. Efficacy of antibody to PNAG against keratitis caused by fungal pathogens. *Invest Ophthalmol Vis Sci*. 2016;57:6797–6804.
14. Langmead B, Salzberg SL. Fast gapped-read alignment with Bowtie 2. *Nat Methods*. 2012;9:357–359.
15. Trapnell C, Roberts A, Goff L, et al. Differential gene and transcript expression analysis of RNA-Seq experiments with TopHat and Cufflinks. *Nat Protoc*. 2012;7:562–578.
16. Planet E, Attolini CS, Reina O, Flores O, Rossell D. htSeqTools: high-throughput sequencing quality control, processing and visualization in R. *Bioinformatics*. 2012;28:589–590.
17. Wang L, Feng Z, Wang X, Wang X, Zhang X. DEGseq: an R package for identifying differentially expressed genes from RNA-Seq data. *Bioinformatics*. 2010;26:136–138.
18. Kanehisa M, Goto S, Kawashima S, Okuno Y, Hattori M. The KEGG resource for deciphering the genome. *Nucleic Acids Res*. 2004;32:D277–D280.

19. Koressaar T, Remm M. Enhancements and modifications of primer design program Primer3. *Bioinformatics*. 2007;23:1289–1291.
20. Untergasser A, Cutcutache I, Koressaar T, et al. Primer3–new capabilities and interfaces. *Nucleic Acids Res*. 2012;40:e115.
21. Rajavelu P, Chen G, Xu Y, Kitzmiller JA, Korfhagen TR, Whitsett JA. Airway epithelial SPDEF integrates goblet cell differentiation and pulmonary Th2 inflammation. *J Clin Invest*. 2015;125:2021–2031.
22. Xu J, Flaczyk A, Neal LM, et al. Scavenger receptor MARCO orchestrates early defenses and contributes to fungal containment during cryptococcal infection. *J Immunol*. 2017;198:3548–3557.
23. Maler MD, Nielsen PJ, Stichling N, et al. Key role of the scavenger receptor MARCO in mediating adenovirus infection and subsequent innate responses of macrophages. *mBio*. 2017;8:e00670–17.
24. Karmakar M, Sun Y, Hise AG, Rietsch A, Pearlman E. Cutting edge: IL-1beta processing during *Pseudomonas aeruginosa* infection is mediated by neutrophil serine proteases and is independent of NLRC4 and caspase-1. *J Immunol*. 2012;189:4231–4235.
25. Kankkunen P, Teirila L, Rintahaka J, Alenius H, Wolff H, Matikainen S. (1,3)-Beta-glucans activate both Dectin-1 and NLRP3 inflammasome in human macrophages. *J Immunol*. 2010;184:6335–6342.
26. Zhang J, Zhao G, Lin J, et al. Role of PTX3 in corneal epithelial innate immunity against *Aspergillus fumigatus* infection. *Exp Eye Res*. 2018;167:152–162.
27. Zhu K, Mu H, Pi B. Regulatory effect of caspase-11 on interleukin-1beta in the fungal keratitis. *Pak J Pharm Sci*. 2016;29:2327–2334.
28. Che C, Li C, Lin J, et al. Wnt5a contributes to Dectin-1 and LOX-1 induced host inflammatory response signature in Aspergillus fumigatus keratitis. *Cell Signal*. 2018;52:103–111.
29. Chwa M, Atilano SR, Hertzog D, et al. Hypersensitive response to oxidative stress in keratoconus corneal fibroblasts. *Invest Ophthalmol Vis Sci*. 2008;49:4361–4369.
30. Gao JR, Qin XJ, Jiang H, Wang T, Song JM, Xu SZ. Screening and functional analysis of differentially expressed genes in chronic glomerulonephritis by whole genome microarray. *Gene*. 2016;589:72–80.
31. Kim YG, Kim M, Kang JH, et al. Transcriptome sequencing of gingival biopsies from chronic periodontitis patients reveals novel gene expression and splicing patterns. *Hum Genomics*. 2016;10:28.
32. Martinelli E, Tharinger H, Frank I, et al. HSV-2 infection of dendritic cells amplifies a highly susceptible HIV-1 cell target. *PLoS Pathog*. 2011;7:e1002109.
33. Kale SD, Ayubi T, Chung D, et al. Modulation of immune signaling and metabolism highlights host and fungal transcriptional responses in mouse models of invasive pulmonary aspergillosis. *Sci Rep*. 2017;7:17096.
34. Wang Y, Liu T, Gong H, et al. Gene profiling in murine corneas challenged with *Aspergillus fumigatus*. *Mol Vis*. 2007;13:1226–1233.
35. Li ZY, Chen ZL, Zhang T, Wei C, Shi WY. TGF-β and NF-κB signaling pathway crosstalk potentiates corneal epithelial senescence through an RNA stress response. *Aging*. 2016;8:2337–2354.
36. Kimura K, Orita T, Morishige N, Nishida T, Sonoda KH. Role of the JNK signaling pathway in downregulation of connexin43 by TNF-α in human corneal fibroblasts. *Curr Eye Res*. 2013;38:926–932.
37. Zhang W, Chen J, Fu Y, Fan X. The signaling pathway involved in the proliferation of corneal endothelial cells. *J Recept Signal Transduct Res*. 2015;35:585–591.
38. Qin XH, Ma X, Fang SF, Zhang ZZ, Lu JM. IL-17 produced by Th17 cells alleviates the severity of fungal keratitis by suppressing CX43 expression in corneal peripheral vascular endothelial cells. *Cell Cycle*. 2019;18:274–287.
39. Sabater AL, Andreu EJ, Garcia-Guzman M, et al. Combined PI3K/Akt and Smad2 activation promotes corneal endothelial cell proliferation. *Invest Ophthalmol Vis Sci*. 2017;58:745–754.
40. Yao B, Wang S, Xiao P, Wang Q, Hea Y, Zhang Y. MAPK signaling pathways in eye wounds: multifunction and cooperation. *Exp Cell Res*. 2017;359:10–16.
41. Taylor PR, Roy S, Meszaros EC, et al. JAK/STAT regulation of *Aspergillus fumigatus* corneal infections and IL-6/23-stimulated neutrophil, IL-17, elastase, and MMP9 activity. *J Leukoc Biol*. 2016;100:213–222.
42. Poon MW, Yan L, Jiang D, et al. Inhibition of RAP1 enhances corneal recovery following alkali injury. *Invest Ophthalmol Vis Sci*. 2015;56:711–721.
43. Mwaikambo BR, Yang C, Chemtob S, Hardy P. Hypoxia up-regulates CD36 expression and function via hypoxia-inducible factor-1- and phosphatidylinositol 3-kinase-dependent mechanisms. *J Biol Chem*. 2009;284:26695–26707.
44. Makino Y, Uenishi R, Okamoto K, et al. Transcriptional up-regulation of inhibitory PAS domain protein gene expression by hypoxia-inducible factor 1 (HIF-1): a negative feedback regulatory circuit in HIF-1-mediated signaling in hypoxic cells. *J Biol Chem*. 2007;282:14073–14082.
45. Zaidi T, Mowrey-McKee M, Pier GB. Hypoxia increases corneal cell expression of CFTR leading to increased *Pseudomonas aeruginosa* binding, internalization, and initiation of inflammation. *Invest Ophthalmol Vis Sci*. 2004;45:4066–4074.
46. Zhang Y, Yeh LK, Zhang S, et al. Wnt/β-catenin signaling modulates corneal epithelium stratification via inhibition of Bmp4 during mouse development. *Development*. 2015;142:3383–3393.
47. Kabza M, Karolak JA, Rydzanicz M, Szcześniak MW, Nowak DM, Ginter-Matuszewska B. Collagen synthesis disruption and downregulation of core elements of TGF-β, Hippo, and Wnt pathways in keratoconus corneas. *Eur J Hum Genet*. 2017;25:582–590.
48. Ferreira R, Wong R, Schlichter LC. KCa3.1/IK1 channel regulation by cGMP-dependent protein kinase (PKG) via reactive oxygen species and CaMKII in microglia: an immune modulating feedback system? *Front Immunol*. 2015;6:153.

Investigative Ophthalmology & Visual Science